Article

Wideband High-Selectivity SIW Filtering Antenna with Controllable Radiation Nulls

Zhongbao Wang[1, 2] (ID), Xinhong Liu[2] (ID), Hongmei Liu[2] (ID), Shaojun Fang[2] (ID)

[1]*Liaoning Key Laboratory of Radio Frequency and Big Data for Intelligent Applications, Liaoning Technical University, Huludao, Liaoning 125105, China. wangzb@dlmu.edu.cn*

[2]*School of Information Science and Technology, Dalian Maritime University, Dalian, Liaoning116026, China. 24130703@qq.com, lhm323@dlmu.edu.cn, fangshj@dlmu.edu.cn*

Abstract—**A novel wideband high-selectivity substrate-integrated-waveguide (SIW) filtering antenna with controllable radiation nulls is proposed. This antenna is composed of a two-layered SIW resonator, two radiating slots on the top layer, and two coupling slots on the middle layer. A vertical SMA connector is located at the bottom and feeds two SIW cavities simultaneously. By adjusting the parameters of these slots, three radiation nulls will be achieved, and two radiation nulls can be easily controlled. For demonstration, one prototype of the filtering antenna is fabricated and measured. Measurement results show that the fractional bandwidth for $|S_{11}| < -10$ dB is 8.9% (3.86–4.23 GHz), the gain is 6.08 dBi at center frequency 4.05 GHz, three radiation nulls are achieved at 3.7 GHz, 4.3 GHz, and 5.19 GHz, respectively. The out-of-band skirt selectivities of two sidebands are 150 and 332 dB/GHz, respectively.**

Index Terms—**controllable radiation null; filtering antenna; high selectivity; substrate integrated waveguide.**

I. INTRODUCTION

The need for a compact, low-cost, highly-integrated, and multifunctional RF front-end is a result of modern wireless communication's rapid development. Because of this, filtering antennas simultaneously having radiation function and frequency selectivity have gained popularity. Several filtering antennas have been developed using microstrip designs, which have the benefits of being inexpensive, simple to produce, and compact [1]-[4]. However, the frequency selectivity of these microstrip filtering antennas is limited. Waveguide cavities [5], dielectric resonators [6], and substrate-integrated waveguide (SIW) [7]-[14] are chosen due to their higher Q-factors for enhancing the antenna filtering performance. Among them, SIW slot antennas have received the most attention due to their simple integration with planar circuits recently. A seamless integration of SIW filter with slot antenna was first presented in [7]. However, the filtering antenna in [7] has no radiation null (RN) near the passband, which leads to poor frequency selectivity.

RN is an important indicator of the filtering antenna. In some applications, controllable RNs can improve the flexibility to meet specific suppression requirements. By using a slot etched roughly on the middle of the radiation cavity, two half modes can be excited to achieve one controllable RN. Several filtering antennas have achieved a controllable RN by this method [8], [9]. However, those

can only achieve high selectivity in one sideband. A combination of a half-mode substrate-integrated rectangular cavity and a parasitic patch was proposed in [10]. Two RNs can be realized, but the lower RN is far away from the passband. In addition, the bandwidth is important for the filtering antenna. However, the SIW cavity has a high Q-factor, which makes it difficult to achieve wideband. Good selectivity in both sidebands was achieved in [11], [12], and [14], but those bandwidths are very narrow.

In this paper, a novel filtering antenna with double-layer substrates, two radiating slots on the top copper layer, and two coupling slots on the middle copper layer is proposed, and achieved wideband high-selectivity filtering with controllable radiation nulls. Adjusting the parameters of these slots, three RNs can be achieved, and two RNs near the passband can be easily controlled. For validation, one prototype of the filtering antenna is fabricated and the measurement results are presented.

II. ANTENNA DESIGN

The configuration of the proposed filtering antenna is shown in Fig. 1(a), which is composed of two substrates, three copper layers, multiple metalized vias, and an SMA connector. The two substrates have the same thickness $h = 1.5$ mm, dielectric constant $\varepsilon_r = 2.65$, and loss tangent $\tan\delta = 0.0035$. The SMA probe feeds two SIW cavities simultaneously. Both the top copper layer and middle copper layer have two slots with different sizes and positions. Coupling occurs between upper and lower slots, resulting in radiation nulls. Three RNs will be achieved in this way.
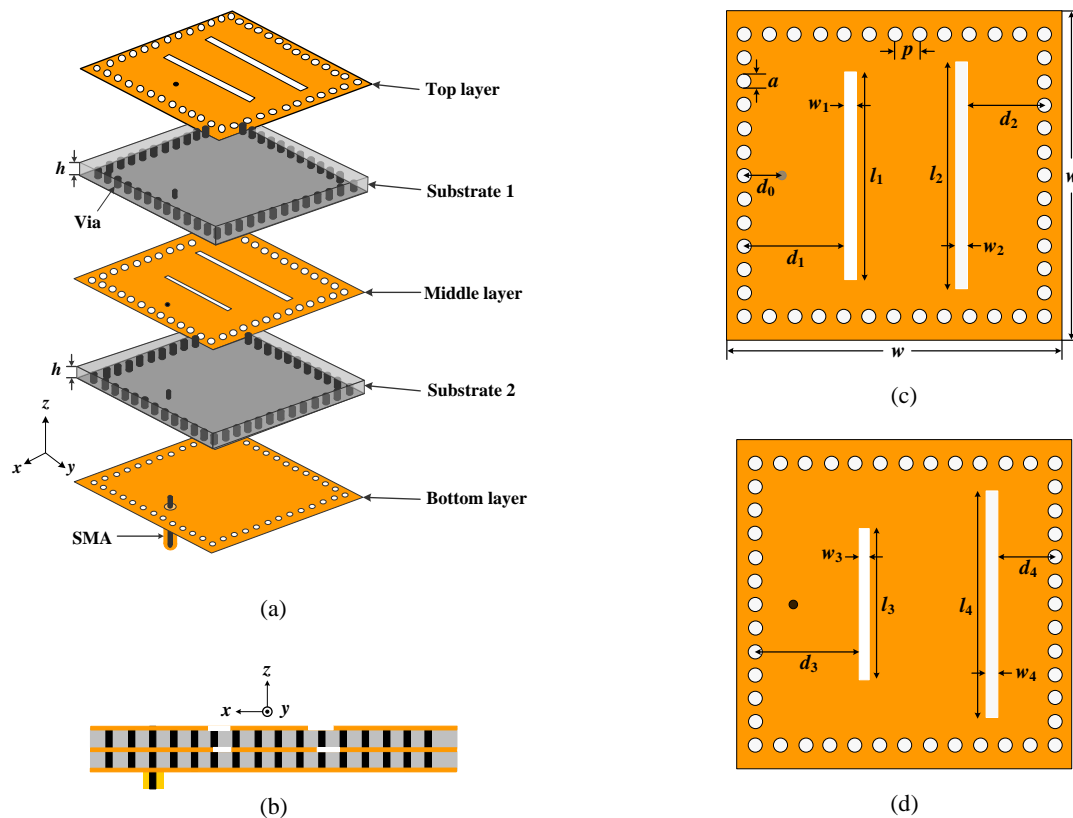

(a)

(b)

(c)

(d)

Fig. 1. Configuration of the proposed filtering antenna. (a) Exploded view. (b) Side view. (c) Top copper layer. (d) Middle copper layer. ($h = 1.5$, $d_0 = 5.9$, $d_1 = 15.3$, $d_2 = 12.2$, $d_3 = 15.5$, $d_4 = 9.6$, $l_1 = 33$, $l_2 = 36.9$, $l_3 = 24.3$, $l_4 = 35.9$, $w = 53$, $w_1 = 1.8$, $w_2 = 1.7$, $w_3 = 1.5$, $w_4 = 1.9$, $p = 3.9$, $a = 2$, all in mm).

A. Antenna Mechanism

To clearly demonstrate the design concept of the proposed filtering antenna, two transitional antennas are analyzed for comparison. The structure of these designs is shown in Fig. 2, including Ant. I (i.e., single-layered SIW antenna with a left slot) and Ant. II (i.e., two-layered SIW antenna with two left slots located respectively on the top and middle copper layers). For comparison, the proposed filtering antenna simultaneously is also shown in Fig. 2. And Ansys HFSS is used to simulate and analyze these antennas. The simulated $|S_{11}|$ of the three antennas and the realized gain at the direction of the $+z$ axis are shown in Fig. 3. It is observed from Fig. 3 that Ant. I has a resonance and a RN, which far away from the resonance frequency. For Ant. II, a new resonance frequency higher than that of Ant. I and a RN near this resonance frequency are added, which is caused by the coupling between the two slots. Furthermore, two more slots on the right of the proposed antenna bring a new resonance and a RN at the lower frequency. By this comparison, it can be seen how the resonances and RNs (RN 1, RN 2, and RN 3) of the proposed antenna realized. The two slots on the right shown in Figs. 1(c) and 1(d) determine RN 1, and the other two slots on the left shown in Figs. 1(c) and 1(d) determine RN 2 and RN 3. Therefore, the position of the RNs can be controlled by adjusting the parameters of each slot.
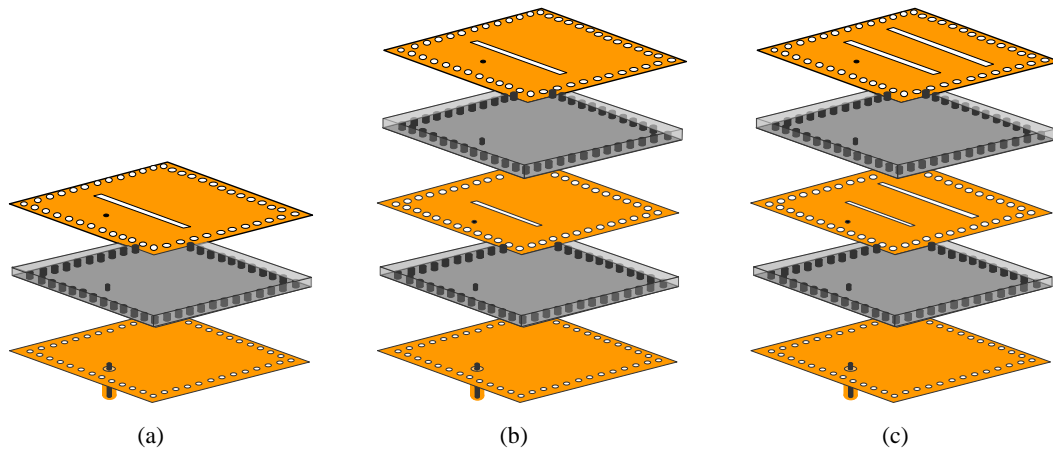

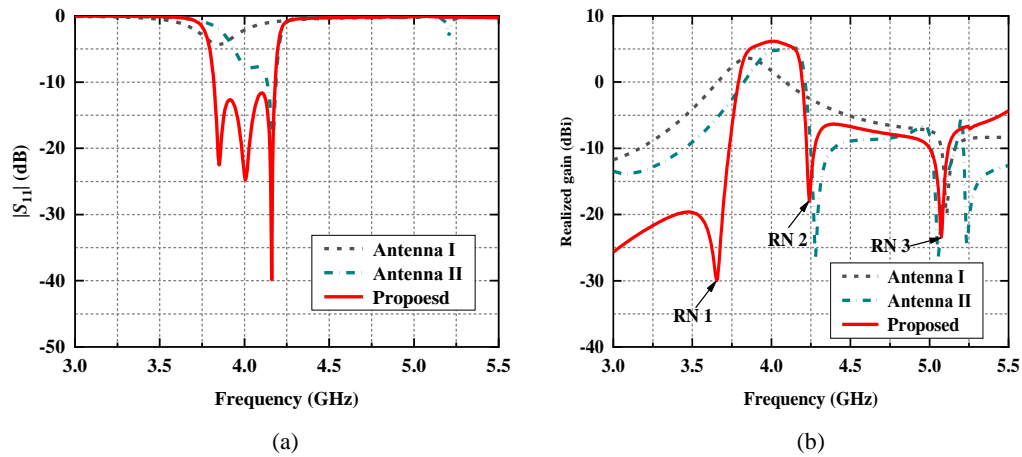Fig. 2. Structure of antennas. (a) Ant. I. (b) Ant. II. (c) Proposed antenna.

(a)   (b)

Fig. 3. Simulated $|S_{11}|$ and gain of the reference and proposed antennas. (a) $|S_{11}|$. (b) Gain.

(a)   (b)   (c)
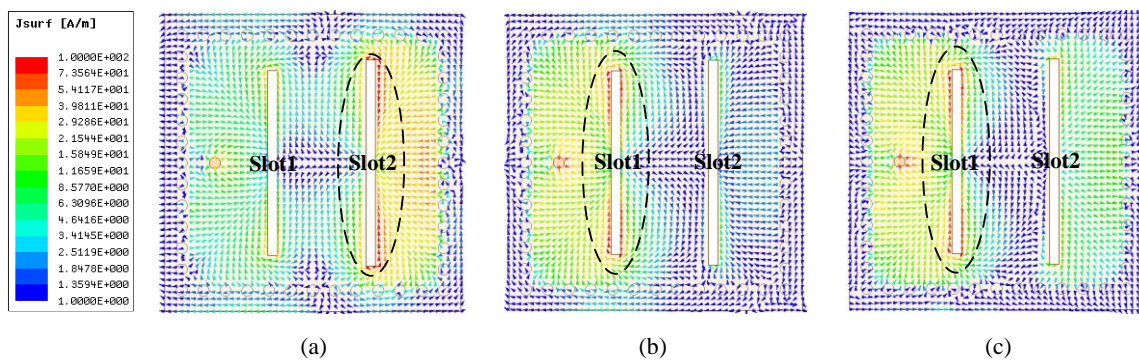
Fig. 4. Current distributions at three resonance frequencies. (a) 3.85 GHz. (b) 4.01 GHz. (c) 4.16 GHz.

To identify the working mechanism, the current distributions on the top copper layer at resonance frequencies are studied. Fig. 4 shows the current distributions at 3.85, 4.01, and 4.16 GHz. It is observed from Fig. 4(a) that stronger surface currents concentrate around radiating Slot 2 (shown by red) on the top copper layer. It is seen from Figs. 4(b) and 4(c), at resonance frequencies 4.01 and 4.16 GHz, stronger surface currents concentrate around radiating Slot 1. Strong surface currents surround Slot 1 and Slot 2, radiating electromagnetic energy outward.

(a)   (b)   (c)
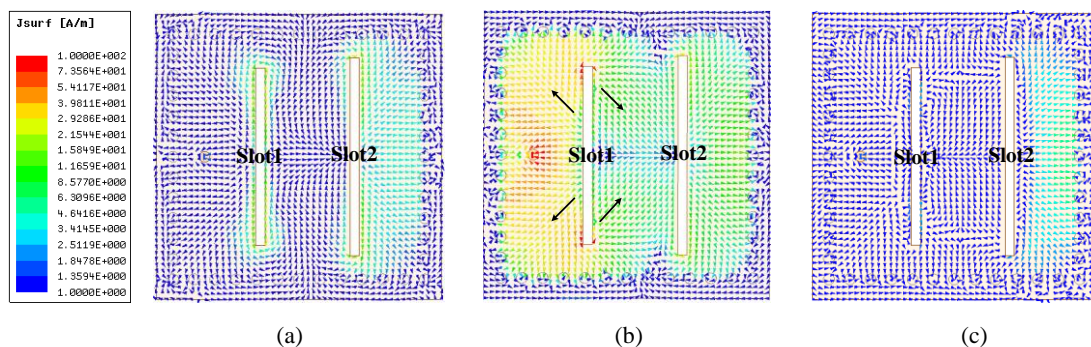
Fig. 5. Current distributions at three RN frequencies. (a) 3.65 GHz. (b) 4.24 GHz. (c) 5.07 GHz.

To identify the RN generation mechanism, the current distributions on the top copper layer of the proposed antenna at RN frequencies are examined. Fig. 5 shows the current distributions at RN frequencies of 3.65, 4.24, and 5.07 GHz. It is seen from Figs. 5(a) and 5(c), at RN frequencies of 3.65

and 5.07 GHz, weak surface currents on the top copper layer can not produce efficient outward radiation, so achieved RN 1 and RN 3. It is observed from Fig. 4(b) that strong surface currents concentrate around the slot 1, but the surface current directions are opposite, producing a radiation cancellation effect, so it is hard to radiate at 4.24 GHz. By adjusting the position and the size of the slots, their resonant frequencies can be changed, and produce this reverse current distribute effect, thereby achieving RN 2.

Fig. 6 shows the radiation patterns at RN frequency of 3.65 GHz. It can be seen that the directivity and realized gain in the direction of the +z axis are −17.4 dBi, and −30.8 dBi, respectively. This indicates that the origin of the radiation null is from the antenna itself, and the input impedance mismatch results in a lower realized gain.
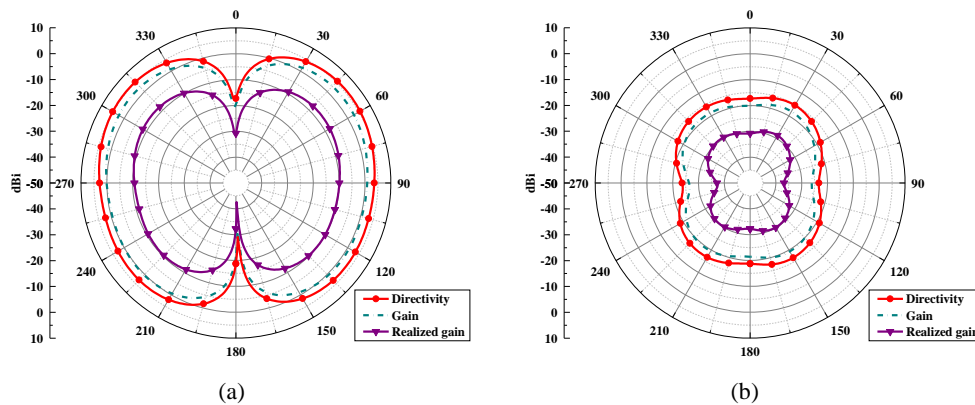

(a)   (b)

Fig. 6. Simulated radiation patterns of the proposed filtering antenna at RN frequency of 3.65 GHz. (a) xoz-plane. (b) yoz-plane.
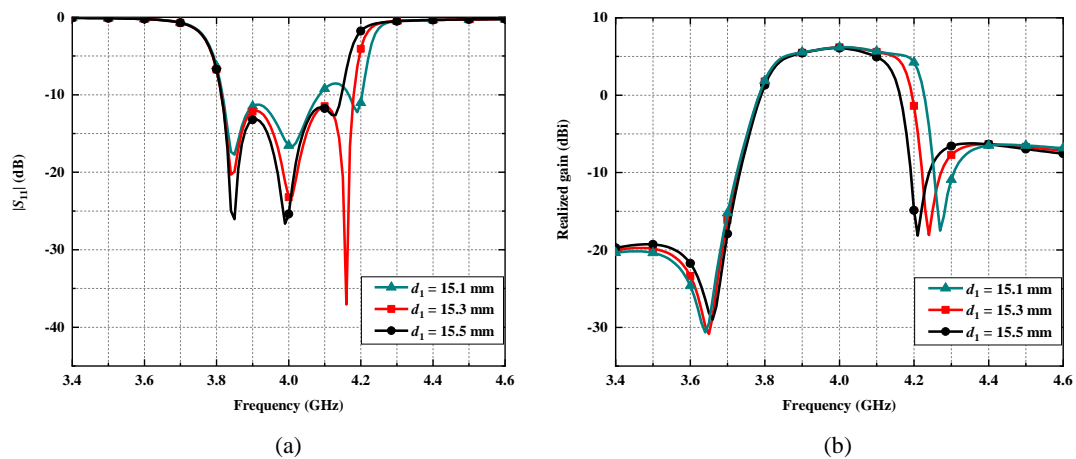

(a)   (b)

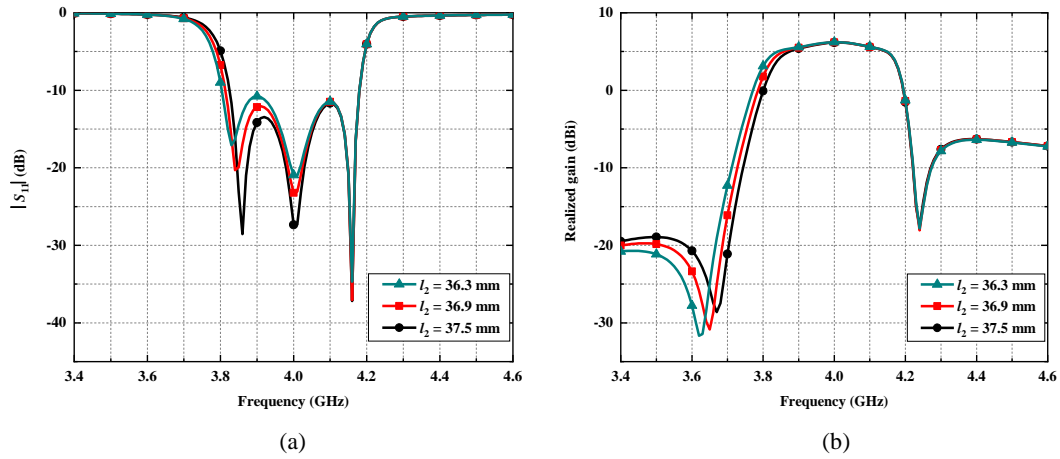Fig. 7. (a) Influence of d_1 on $|S_{11}|$. (b) Influence of d_1 on the realized gain

Fig. 8. (a) Influence of l_2 on $|S_{11}|$. (b) Influence of l_2 on the realized gain

B. Frequency Control of Radiation Nulls

Based on the above analysis, the RN frequencies are decided by the parameters of the slots. Figs. 7–10 show the influences of the slots on $|S_{11}|$ and gain of the proposed antenna. As shown in Fig. 7, with the increase of d_1, RN 2 moves to a lower frequency, but the impedance bandwidth for $|S_{11}| < -10$ dB will reduce. In Fig. 8, with the increase of l_2, RN 1 moves to a higher frequency with impedance matching at 3.9 GHz becomes better.
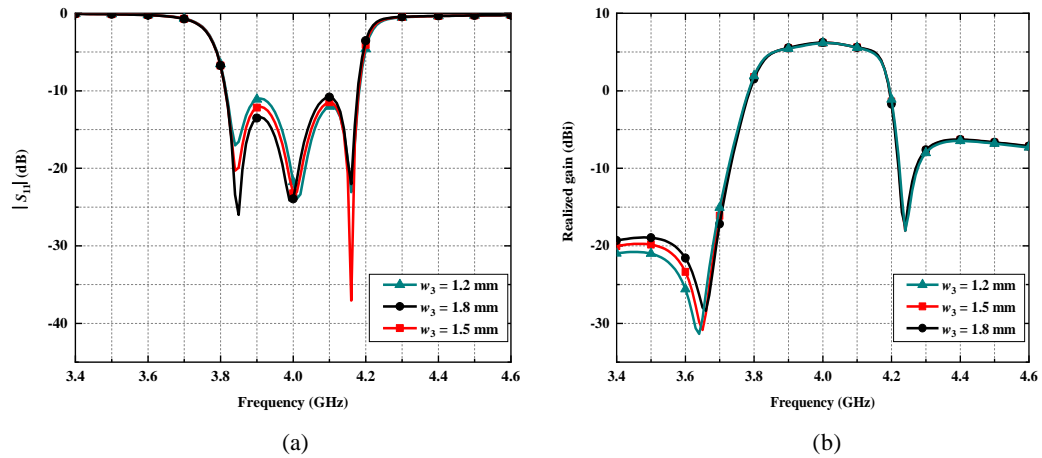

Fig. 9. (a) Influence of w_3 on $|S_{11}|$. (b) Influence of w_3 on the realized gain

In Fig. 9, with the increase of w_3, RN 1 moves to a higher frequency, impedance matching at 3.9 GHz becomes better and 4.1 GHz becomes worse. And as shown in Fig. 10, with the increase of d_4, RN 1 moves to a higher frequency with impedance matching at 3.9 GHz becomes better.
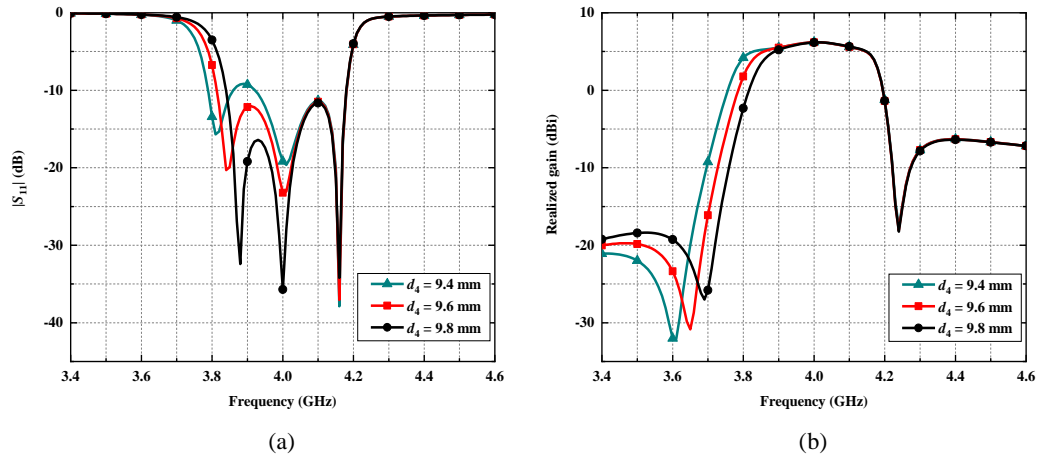
Fig. 10. (a) Influence of d_4 on $|S_{11}|$. (b) Influence of d_4 on the realized gain
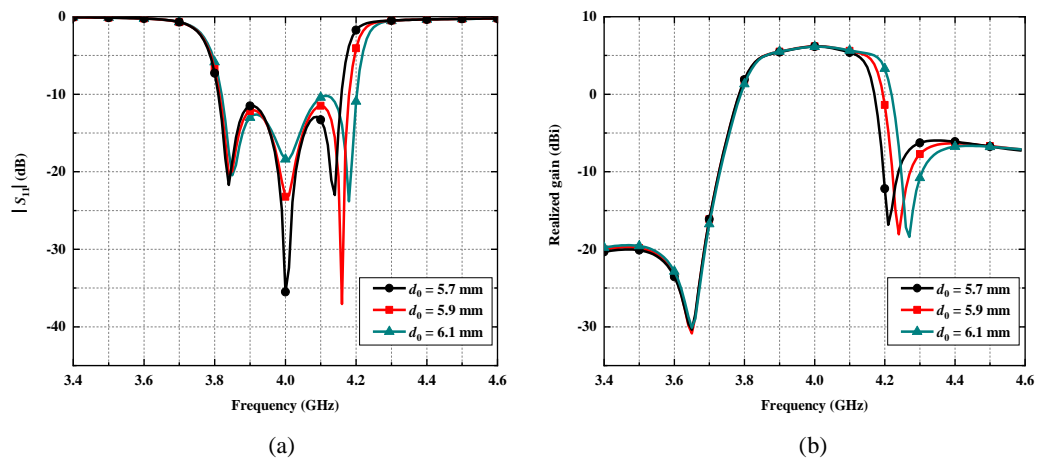

Fig. 11. (a) Influence of d_0 on $|S_{11}|$. (b) Influence of d_0 on the realized gain

The position of the SMA connector also affects impedance matching and RN 2. As shown in Fig. 11, with the increase of d_0, RN 2 moves to a higher frequency with impedance matching at 4.1 GHz becomes worse. Thus, changing the parameter of each slot and the position of the SMA connector can flexibly control the impedance bandwidth and the RN position, achieving controllable RNs.

C. Antenna Design Procedure

Based on the foregoing analysis, the following procedures are suggested to design the proposed SIW filtering antenna.

1) Determine the center frequency and impedance bandwidth according to the design requirements. Obtain the values of relative dielectric constant ε_r and thickness h of the substrate.

2) Setting the dimensions of the two-layered SIW cavity as w is $1.14\lambda_g$, $a = 0.05\lambda_g$, $p = 0.08\lambda_g$. Add feeding probe and set the dimension $d_0 = 0.13\lambda_g$. Adjusting the dimensions of w, a, p and d_0 to get a SIW cavity that satisfies the center frequency.

3) Calculate slot-width $0.04\lambda_g$. Setting the initial dimensions of four slots as $d_1 = 0.33\lambda_g$, $d_2 = 0.27\lambda_g$, $d_3 = 0.33\lambda_g$, $d_4 = 0.21\lambda_g$, $l_1 = 0.72\lambda_g$, $l_2 = 0.80\lambda_g$, $l_3 = 0.53\lambda_g$, $l_4 = 0.78\lambda_g$. Tuning the dimensions of the slots referring to Figs. 7–10.

4) Finally, adjusting each parameter to optimize the design for obtaining good filtering performance and needed bandwidth.

III. IMPLEMENTATION AND PERFORMANCE

For validation, the proposed filtering antenna was fabricated. Fig. 12 shows the photographs of this antenna. To ensure the alignment of the substrates during the antenna assembly, four metal screws with the same size are installed at the four corners of the antenna, as shown in Fig. 12(c). The $|S_{11}|$ was measured using an Agilent N5230A vector network analyzer, and the gain and radiation pattern were measured in a far-field anechoic chamber.
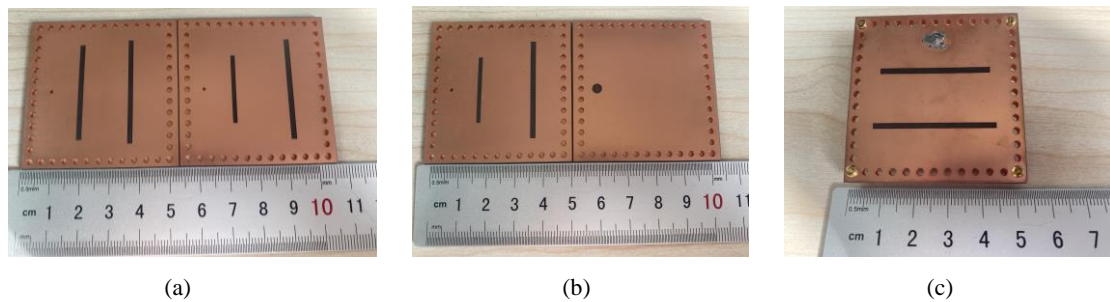

| (a) | (b) | (c) |

Fig. 12. Photographs of the fabricated filtering antenna. (a) Top view of two substrates. (b) Bottom view of two substrates. (c) Overall structure.

Fig. 13 compares the simulated and measured results in detail. It can be seen that the simulated impedance bandwidth for $|S_{11}| < -10$ dB of the proposed filtering antenna is 9.5% (3.81–4.18 GHz), and the measured impedance bandwidth is 8.9% (3.86–4.23GHz). There are some frequency offset between the simulation and measurement results, which are mainly due to the dielectric constant deviation of the substrates, and inevitable introduction of air layer with uncertain thickness between two substrates during fabrication. For the radiation responses, the maximum gain of measurement is 6.08 dBi, three RNs are obtained and located at 3.7 GHz, 4.3 GHz, and 5.19 GHz, respectively. The left out-of-band skirt selectivity is 150 dB/GHz (i.e., $|\alpha_{max} - \alpha_{min}| / |f_z - f_c| = |33 - 3| / |3.7 - 3.9|$ dB/GHz, where α_{max} is the attenuation at the first out-of-band RN and α_{min} is the 3-dB attenuation, f_z and f_c are their corresponding frequencies), and the suppression level is more than 26 dB. The right out-of-band skirt selectivity is 332 dB/GHz, and the suppression level is more than 13.5 dB. A high skirt selectivity in each sideband is achieved, which attributes to the controllable RN 1 and RN 2 that can be tuning close to the passband.
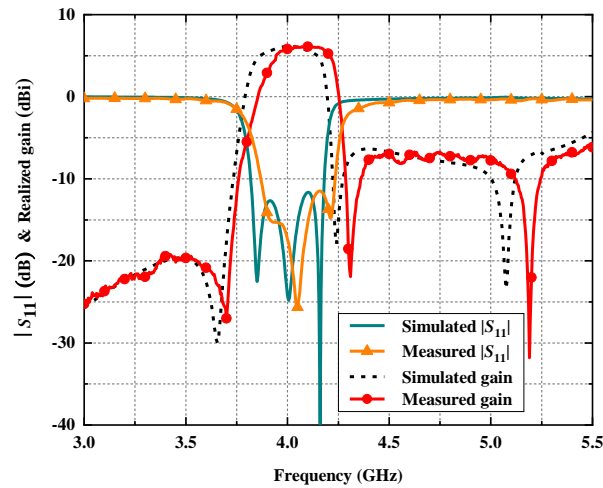
Fig. 13. Simulated and measured |S_{11}| and gain of the proposed filtering antenna.
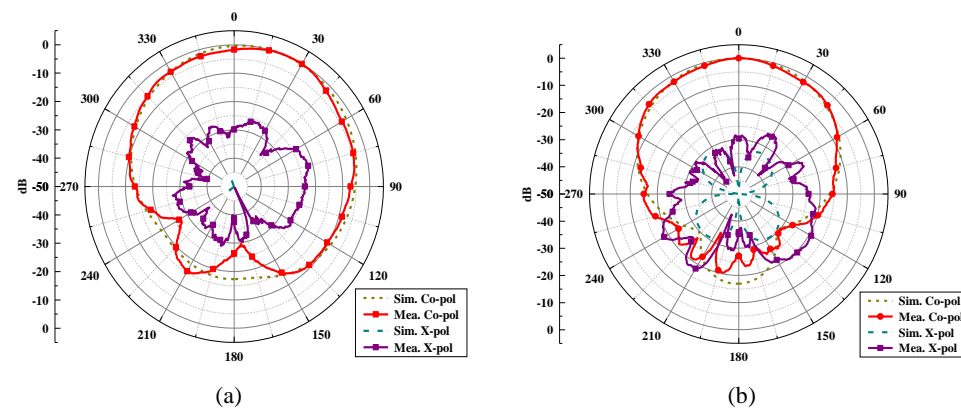

(a)   (b)

Fig. 14. Normalized radiation patterns of the proposed filtering antenna. (a) E-plane. (b) H-plane.

The normalized radiation patterns of proposed filtering antenna at the center frequency are shown in Fig. 14. The measured half-power beam-widths are 75° in the E-plane and 84° in the H-plane. In the half-power beam, good cross-polarization suppression of more than 24 dB is obtained in both planes. Fig. 15 shows the radiation efficiency versus frequency for the proposed filtering antenna. It is observed that the radiation efficiency near the center frequency of 4 GHz is about 91%. Table I compares the proposed filtering antenna with previous works. It can be seen that this work has some advantages in the bandwidth, frequency selectivity, and size. Moreover, the proposed filtering antenna introduces two controllable radiation nulls.
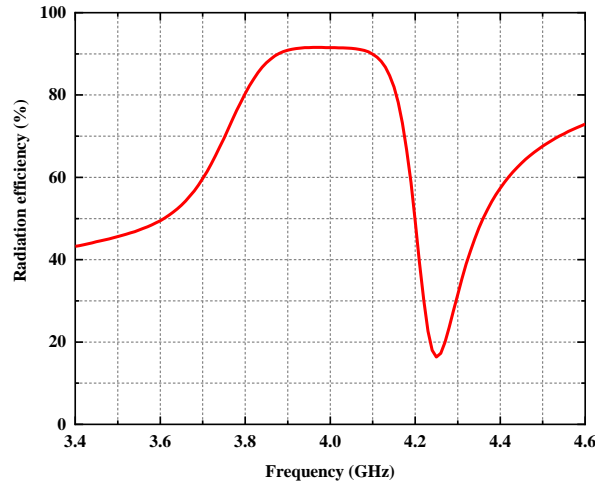
Fig. 15. Simulated radiation efficiency of the proposed filtering antenna.

TABLE I. COMPARISON BETWEEN THE PROPOSED ANTENNA AND THE EXISTING SIW FILTERING ANTENNAS

References	f_0 (GHz)	FBW (%)	Gain (dBi)	NRN (NCRN)	Lower/Upper Selectivity (dB/GHz）	Size (λg × λg)
[8]	4.43	5.4	6.5	1(1)	100/134	1.3×1.2
[9]	3.71	8.3	5.1	1(1)	74/865	1.4×1.0
[10]	2.77	5.1	6.3	2(2)	68/233	1.1×0.8
[11]	5.5	2.6	4.3	2(0)	300/170	1.1×0.7
[12]	5.365	7.6	5.3	2(2)	375/257	1.9×1.6
[13]	31.5	1.6	6.79	2(0)	26/57	3.3×2.5
[14]	5.16	2.5	6.79	4(0)	231/213	1.6×1.5
This work	4.05	8.9	6.08	3(2)	150/332	1.1×1.1

where f_0 is the center frequency, NRN is the number of RNs, and NCRN is the number of controllable RNs. *Lower/upper selectivity is calculated as $|\alpha_{max} - \alpha_{min}| / |f_z - f_c|$, where α_{max} is the attenuation at the first out-of-band RN or 20 dB attenuation if no RN and α_{min} is the 3-dB attenuation, f_z and f_c are their corresponding frequencies.

IV. CONCLUSION

In this paper, a wideband high-selectivity SIW filtering antenna with controllable RNs has been proposed. By the couplings between the radiating slots on the top copper layer and the coupling slots on the middle copper layer, three RNs have been achieved. The positions of radiation nulls can be controlled by adjusting the parameters of each slot to realize high selectivity. One prototype filtering antenna has been fabricated and measured for validation. The proposed antenna has good filtering response and radiation performance, making it perfect for a practical integrated module in a wireless front-end system.

REFERENCES

[1] J. F. Qian, F. C. Chen, Q. X. Chu, Q. Xue, and M. J. Lancaster, "A novel electric and magnetic gap-coupled broadband patch antenna with improved selectivity and its application in MIMO system," *IEEE Trans. Antennas Propag.*, vol. 66, no. 10, pp. 5625-5629, 2018.

[2] B. Zhang and Q. Xue, "Filtering antenna with high selectivity using multiple coupling paths from source/load to resonators," *IEEE Trans. Antennas Propag.*, vol. 66, no. 8, pp. 4320-4325, 2018.

[3] W. Yang, S. Chen, Q. Xue, W. Che, G. Shen, and W. Feng, "Novel filtering method based on metasurface antenna and its application for wideband high-gain filtering antenna with low profile," *IEEE Trans. Antennas Propag.*, vol. 67, no. 3, pp. 1535-1544, 2019.

[4] Y. M. Pan, P. F. Hu, X. Y. Zhang, and S. Y. Zheng, "A low-profile high-gain and wideband filtering antenna with metasurface," *IEEE Trans. Antennas Propag.*, vol. 64, no. 5, pp. 2010-2016, 2016.

[5] F. C. Chen, J. F. Chen, Q. X. Chu, and M. J. Lancaster, "X-band waveguide filtering antenna array with nonuniform feed structure," *IEEE Trans. Microw. Theory Techn.*, vol. 65, no. 12, pp. 4843-4850, 2017.

[6] Y. T. Liu, K. W. Leung, J. Ren, and Y. X. Sun, "Linearly and circularly polarized filtering dielectric resonator antennas," *IEEE Trans. Antennas Propag.*, vol. 67, no. 6, pp. 3629-3640, 2019.

[7] Y. Yusuf, H. Cheng, and X. Gong, "A seamless integration of 3-D vertical filters with highly efficient slot antennas," *IEEE Trans. Antennas Propag.*, vol. 59, no. 11, pp. 4016-4022, 2011.

[8] P. K. Li, C. J. You, H. F. Yu, X. Li, Y. W. Yang, and J. H. Deng, "Codesigned high-efficiency single-layered substrate integrated waveguide filtering antenna with a controllable radiation null," *IEEE Antennas Wireless Propag. Lett.*, vol. 17, no. 2, pp. 295-298, 2018.

[9] R. Lovato and X. Gong, "A third-order SIW-integrated filter/antenna using two resonant cavities," *IEEE Antennas Wireless Propag. Lett.*, vol. 17, no. 3, pp. 505-508, 2018.

[10] K. Z. Hu, M. C. Tang, D. Li, Y. Wang, and M. Li, "Design of compact, single-layered substrate integrated waveguide filtenna with parasitic patch," *IEEE Trans. Antennas Propag.*, vol. 68, no. 2, pp. 1134-1139, 2020.

[11] K. Dhwaj, J. M. Kovitz, H. Tian, L. J. Jiang, and T. Itoh, "Half-mode cavity-based planar filtering antenna with controllable transmission zeroes," *IEEE Antennas Wireless Propag. Lett.*, vol. 17, no. 5, pp. 833-836, 2018.

[12] H. Y. Xie, B. Wu, Y. L. Wang, C. Fan, J. Z. Chen, and T. Su, "Wideband SIW filtering antenna with controllable radiation nulls using dual-mode cavities," *IEEE Antennas Wireless Propag. Lett.*, vol. 20, no. 9, pp. 1799-1803, 2021.

[13] H. Chu, C. Jin, J. X. Chen, and Y. X. Guo, "A 3-D millimeter-wave filtering antenna with high selectivity and low cross-polarization," *IEEE Trans. Antennas Propag.*, vol. 63, no. 5, pp. 2375-2380, 2015.

[14] L. Li, D. Pang, Y. Feng, Q. Wang, and Z. Lei, "A low-profile third-order half-mode SIW filtering antenna with low H-plane cross polarization and good sideband suppression," *IEEE Antennas Wireless Propag. Lett.*, vol. 18, no. 12, pp. 2503-2507, 2019.